

Fourier Analysis-based Iterative Combinatorial Auctions

Jakob Weissteiner,¹ Chris Wendler,² Sven Seuken,¹ Ben Lubin,³ Markus Püschel²

¹University of Zurich,

²ETH Zurich,

³Boston University

weissteiner@ifi.uzh.ch, chris.wendler@inf.ethz.ch, seuken@ifi.uzh.ch, blubin@bu.edu, pueschel@inf.ethz.ch

Abstract

Recent advances in Fourier analysis have brought new tools to efficiently represent and learn set functions. In this paper, we bring the power of Fourier analysis to the design of iterative combinatorial auctions. The key idea is to approximate the bidders' value functions using Fourier-sparse set functions, which can be computed using a relatively small number of queries. Since this number is still too large for real-world auctions, we propose a novel hybrid auction design: we first use neural networks to learn bidders values and then apply Fourier analysis to those learned representations. On a technical level, we formulate a Fourier transform-based winner determination problem and derive its mixed integer program formulation. Based on this, we devise an iterative mechanism that asks Fourier-based queries. Our experimental evaluation shows that our hybrid auction leads to a fairer distribution of social welfare among bidders and significantly reduces runtime, while matching the economic efficiency of state-of-the-art auction designs. With this paper, we are the first to leverage Fourier analysis in combinatorial auction design and lay the foundation for future work in this area.

1 Introduction

Combinatorial auctions (CAs) are used to allocate multiple heterogeneous items to bidders. CAs are particularly useful in domains where bidders' preferences exhibit *complementarities* and *substitutabilities* as they allow bidders to submit bids on *bundles* of items rather than on individual items.

Because the space of bundles grows exponentially in the number of items, it is impossible for bidders to report values for all bundles in settings with more than a modest number of items. Thus the design of a parsimonious preference elicitation is important for the practical design of CAs.

For general value functions, Nisan and Segal (2006) have shown that to achieve full efficiency in a CA, exponential communication in the number of items is needed in the worst case. Therefore, practical CA designs cannot provide efficiency guarantees in large domains. Instead, recent proposals for CAs have focused on *iterative combinatorial auctions* (ICAs) where the auctioneer interacts with bidders over multiple rounds, eliciting a *limited* amount of information, aiming to find a highly efficient allocation.

ICAs have found widespread application in practice (Ausubel and Cramton 2011; Cramton 2013). For example, for the sale of spectrum licenses, the combinatorial clock

auction (CCA) (Ausubel, Cramton, and Milgrom 2006) has generated billions of dollars in total revenue over the past few years (Ausubel and Baranov 2017). Therefore, increasing the efficiency of such real-world ICAs by only 1–2% points translates into monetary gains of millions of dollars.

1.1 Machine Learning-based Auction Design

Recently, researchers have successfully used machine learning (ML) to improve the performance of CAs. Early work by Blum et al. (2004) and Lahaie and Parkes (2004) laid the foundation for this by studying the relationship between computational learning theory and preference elicitation in CAs. Dütting et al. (2019) and Rahme et al. (2020) used neural networks (NNs) to learn auction mechanisms from data, following the automated mechanism design paradigm. Brero, Lahaie, and Seuken (2019) introduced a Bayesian ICA using probabilistic price updates to achieve faster convergence. Most related to the present paper is the work by Brero, Lubin, and Seuken (2017; 2018; 2020), who developed a value-query-based ML-powered ICA using support vector regressions (SVRs) that achieves even higher efficiency than the CCA. In follow-up work, Weissteiner and Seuken (2020) extended their mechanism to NNs, further increasing the efficiency. However, especially in large domains, it remains a challenge to find the efficient allocation while keeping the elicitation cost for bidders low. Therefore, even state-of-the-art approaches suffer from significant efficiency losses and often result in unfair allocations, highlighting the need for better preference elicitation algorithms.

1.2 Combining Fourier Analysis and CAs

The goal of preference elicitation in CAs is to learn bidders' value functions using only a small number of queries. Mathematically, value functions are *set functions*, which are in general exponentially large objects that are notoriously hard to represent or learn. In this paper, we leverage Fourier analysis for set functions (Bernasconi, Codenotti, and Simon 1996; O'Donnell 2014; Püschel 2018) to control for this complexity. In particular, we consider *Fourier-sparse approximations*, which are represented by a small number of parameters. These parameters are the non-zero Fourier coefficients (FCs) obtained by a base change with the Fourier transform (FT). We use the framework by Püschel and

Wendler (2020), which contains new FTs beyond the classical Walsh-Hadamard transform (WHT) (Bernasconi, Codenotti, and Simon 1996), providing additional flexibility.

Until recently, methods for learning Fourier-sparse set functions were focused solely on the WHT, and they placed assumptions on bidders' value functions that are too restrictive for large CAs. For example, the method by Stobbe and Krause (2012) requires a superset of the non-zero FCs to be known and the method by Scheibler, Haghighatshoar, and Vetterli (2015) places uniform randomness assumptions on the non-zero FCs and their positions.

However, recently Amrollahi et al. (2019) proposed a novel algorithm that can approximate general set functions by WHT-sparse ones. Thus, it is suitable for large CAs and we use it in this work.

1.3 Our Contribution

Our main contribution in this paper is to bring the power of Fourier analysis to CA design. In particular, we formulate *FT-based winner determination problems (WDPs)* and derive associated mixed integer programs (MIPs) for the various notions of FTs. Our MIPs allow for the efficient solution of the FT-based WDP. Thus, they provide the foundation for using Fourier-sparse approximations in auction design.

We first show experimentally that the WHT performs best among the FTs in terms of reconstruction error. As an initial approach to leveraging the WHT, we develop a WHT-based allocation rule. However, this requires too many (several thousand) queries for direct use in CAs. To overcome this issue, we propose a practical hybrid ICA mechanism based on NNs and Fourier analysis. The key idea is to compute Fourier-sparse approximations of NN-based bidder representations, enabling us to keep the number of queries small.

Our experiments show that our hybrid ICA matches the economic efficiency of state-of-the-art mechanisms, but yields a significant computational speedup and fairer allocations. Overall, our results show that leveraging Fourier analysis in CA design is a promising new research direction.

2 Preliminaries

In this section, we present our formal model and review the ML-based ICA by Brero, Lubin, and Seuken (2020).

2.1 Formal Model for ICAs

We consider a CA with n bidders and m indivisible items. Let $N := \{1, \dots, n\}$ and $M := \{1, \dots, m\}$ denote the set of bidders and items, respectively. We denote with $x \in \mathcal{X} := \{0, 1\}^m$ a bundle of items represented as an indicator vector, where $x_j = 1$ iff item $j \in M$ is contained in x . Bidders' true preferences over bundles are represented by their (private) value functions $v_i : \mathcal{X} \rightarrow \mathbb{R}_+$, $i \in N$, i.e., $v_i(x)$ represents bidder i 's true value for bundle x .

By $a := (a_1, \dots, a_n) \in \mathcal{X}^n$ we denote an allocation of bundles to bidders, where a_i is the bundle bidder i obtains. We denote the set of *feasible* allocations by $\mathcal{F} := \{a \in \mathcal{X}^n : \sum_{i \in N} a_{ij} \leq 1, \forall j \in M\}$. The (true) *social welfare* of an allocation a is defined as $V(a) :=$

$\sum_{i \in N} v_i(a_i)$. We let $a^* \in \operatorname{argmax}_{a \in \mathcal{F}} V(a)$ be a social-welfare maximizing, i.e., *efficient*, allocation. The efficiency of any $a \in \mathcal{F}$ is measured in terms of a^* by $V(a)/V(a^*)$.

An ICA *mechanism* defines how the bidders interact with the auctioneer and how the final allocation and payments are determined. We denote a bidder's (possibly untruthful) reported value function by $\hat{v}_i : \mathcal{X} \rightarrow \mathbb{R}_+$. In this paper, we consider ICAs that ask bidders to iteratively report their values $\hat{v}_i(x)$ for particular bundles x selected by the mechanism. A finite set of such reported bundle-value pairs of bidder i is denoted as $R_i := \{(x^{(l)}, \hat{v}_i(x^{(l)}))\}$, $x^{(l)} \in \mathcal{X}$. Let $R := (R_1, \dots, R_n)$ denote the tuple of reported bundle-value pairs obtained from all bidders and let $R_{-i} := (R_1, \dots, R_{i-1}, R_{i+1}, \dots, R_n)$. We define the *reported social welfare* of an allocation a given R as

$$\hat{V}(a|R) := \sum_{i \in N: (a_i, \hat{v}_i(a_i)) \in R_i} \hat{v}_i(a_i), \quad (1)$$

where the condition $(a_i, \hat{v}_i(a_i)) \in R_i$ ensures that only values for reported bundles contribute to the sum. Finally, the optimal allocation $a_R^* \in \mathcal{F}$ given reports R is defined as

$$a_R^* \in \operatorname{argmax}_{a \in \mathcal{F}} \hat{V}(a|R). \quad (2)$$

In the mechanisms we consider in this paper, the *final outcome* is only computed based on the reported values R . Specifically, the mechanism determines an allocation $a_R^* \in \mathcal{F}$ and charges payments $p = (p_1, \dots, p_n) \in \mathbb{R}_+^n$. We assume that bidders have quasilinear utilities.

As the auctioneer can generally only ask each bidder i for a limited number of bundle-value pairs R_i (e.g., 500), the mechanism needs a sophisticated preference elicitation algorithm, with the goal of finding a highly efficient allocation with a limited number of value queries. More formally: *given a cap κ on the number of value queries in an ICA, elicit from each bidder $i \in N$ a set of reported bundle-value pairs R_i with $|R_i| \leq \kappa$ such that the resulting efficiency of a_R^* is maximized, i.e., $R \in \operatorname{argmax}_{R: |R_i| \leq \kappa} V(a_R^*)/V(a^*)$.*

2.2 A Machine Learning powered ICA

We now review the *machine learning-powered combinatorial auction (MLCA)* introduced by Brero, Lubin, and Seuken (2020). Instead of using SVRs as the ML algorithm, we describe MLCA using NNs \mathcal{N}_i (a variation introduced by Weissteiner and Seuken (2020)).

At the core of MLCA is a query module (Algorithm 1), which, for each bidder $i \in I$, determines a new value query q_i . First, in the *estimation step* (Line 1), NNs are used to learn bidders' valuations from reports R_i . Next, in the *optimization step* (Line 2), a *NN-based WDP* is solved to find a candidate q of queries. See Weissteiner and Seuken (2020) for details on the NN-based *estimation* and *optimization step*. Finally, if q_i has already been queried before (Lines 4–8), another, more restricted, NN-based WDP (Line 6) is solved and q_i is updated. This ensures that all final queries q are new. In Algorithm 2, we present MLCA in a slightly abbreviated form. MLCA proceeds in rounds until a maximum number of queries per bidder Q^{\max} is reached. In each

Algorithm 1: NN-QUERY MODULE (Brero et al. 2020)

Function : $NextQueries(I, R)$
Inputs : Index set of bidders I and reported values R
Parameters: Neural networks $\mathcal{N}_i : \mathcal{X} \rightarrow \mathbb{R}_+$, $i \in N$

- 1 **foreach** $i \in I$ **do** Fit \mathcal{N}_i on R_i : $\mathcal{N}_i[R_i]$ ▷ Estimation step
- 2 Solve $q \in \operatorname{argmax}_{a \in \mathcal{F}} \sum_{i \in I} \mathcal{N}_i[R_i](a_i)$ ▷ Optimization step
- 3 **foreach** $i \in I$ **do**
- 4 **if** $q_i \in R_i$ **then** ▷ Bundle already queried
- 5 Define $\mathcal{F}' := \{a \in \mathcal{F} : a_i \neq x, \forall x \in R_i\}$
- 6 Resolve $q' \in \operatorname{argmax}_{a \in \mathcal{F}'} \sum_{l \in I} \mathcal{N}_l[R_l](a_l)$
- 7 Update $q_i = q'_i$
- 8 **end**
- 9 **end**
- 10 **return** profile of new queries $q = (q_1, \dots, q_n)$

round, it calls Algorithm 1 n times: once including all bidders (Line 6, *main economy*) and $n - 1$ times excluding one bidder (Lines 7–9, *marginal economies*). At the end of each round, the mechanism receives reports R^{new} from all bidders for the newly generated queries q^{new} , and updates the overall elicited reports R (Lines 10–12). In Lines 15–16, MLCA computes an allocation a_R^* that maximizes the *reported social welfare* and determines VCG payments p (see the technical appendix Section A.1 for details on p).

Brero, Lubin, and Seuken (2020) argue that MLCA, while not strategyproof, provides good incentives for bidders to report truthfully. Their incentive analysis also applies to the hybrid ICA we propose in Section 6.1. These arguments notwithstanding, mechanisms only have access to bidders' reported value functions \hat{v}_i not their true function v_i , and we therefore maintain this distinction in our notation.

Algorithm 2: MLCA (Brero et al. 2020)

Params: $Q^{\text{init}}, Q^{\text{max}}$ initial and max #queries per bidder

- 1 **foreach** $i \in N$ **do**
- 2 Randomly draw initial reports R_i with $|R_i| = Q^{\text{init}}$
- 3 **end**
- 4 Set $t = 1$
- 5 **while** $t \leq \lfloor (Q^{\text{max}} - Q^{\text{init}})/n \rfloor$ **do** ▷ Round iterator
- 6 $q^{\text{new}} \leftarrow NextQueries(N, R)$ ▷ Main economy queries
- 7 **foreach** bidder $i \in N$ **do** ▷ Marginal economy queries
- 8 $q^{\text{new}} \leftarrow NextQueries(N \setminus \{i\}, R_{-i})$
- 9 **end**
- 10 **foreach** bidder $i \in N$ **do**
- 11 Receive reports R_i^{new} for q_i^{new} , set $R_i = R_i \cup R_i^{\text{new}}$
- 12 **end**
- 13 $t = t + 1$
- 14 **end**
- 15 Given elicited reports R compute a_R^* as in (2)
- 16 Given elicited reports R compute VCG-payments p
- 17 **return** final allocation a_R^* and payments p

3 Fourier Analysis of Value Functions

In this section, we show how to apply Fourier analysis to bidders' value functions and provide the theoretical foundation of Fourier transform-based WDPs.

Classic Fourier analysis decomposes an audio signal or image into an orthogonal set of sinusoids of different frequencies. Similarly, the classical Fourier analysis for *set functions* (i.e., functions mapping each subset of a discrete set to a scalar) decomposes a set function into an orthogonal set of Walsh functions (Bernasconi, Codenotti, and Simon 1996; O'Donnell 2014), which are piecewise constant with values 1 and -1 only. Recent work by Püschel and Wendler (2020) extends the Fourier analysis for set functions with several novel forms of set Fourier transforms (FTs). Importantly, because bidders' value functions are set functions, they are amenable to this type of Fourier analysis, and it is this connection that we will leverage in our auction design.

Sparsity. The motivation behind our approach is that we expect bidders' value functions to be *sparse*, meaning that their preferences can be described with much less data than is contained in the (exponentially-sized) full value function. While this sparsity may be difficult to uncover when looking at bidders' value reports, it may reveal itself in the Fourier domain (where then most Fourier coefficients (FCs) are zero). As all FTs are changes of basis, each FT provides us with a new *lens on the bidder's value function*, potentially revealing structure and thus reducing dimensionality.

Set function Fourier transform. We now provide a formal description of FTs for reported value functions \hat{v}_i . To do so, we represent \hat{v}_i as a vector $(\hat{v}_i(x))_{x \in \mathcal{X}}$. Specializing to transforming such \hat{v}_i , all known FTs can be represented by a certain matrix $F \in \{-1, 0, 1\}^{2^m \times 2^m}$ with the form:

$$\phi_{\hat{v}_i}(y) = (F\hat{v}_i)(y) = \sum_{x \in \mathcal{X}} F_{y,x} \hat{v}_i(x). \quad (3)$$

The corresponding inverse transform F^{-1} is thus:

$$\hat{v}_i(x) = (F^{-1}\phi_{\hat{v}_i})(x) = \sum_{y \in \mathcal{X}} F_{x,y}^{-1} \phi_{\hat{v}_i}(y). \quad (4)$$

We call $\phi_{\hat{v}_i}(y) \in \mathbb{R}$ the *Fourier coefficient* at frequency y . Formally, a value function is *Fourier-sparse* if $|\operatorname{supp}(\phi_{\hat{v}_i})| = |\{y \in \mathcal{X} : \phi_{\hat{v}_i}(y) \neq 0\}| \ll 2^m$. We call $\operatorname{supp}(\phi_{\hat{v}_i})$ the *Fourier support* of \hat{v}_i .

Classically, the WHT is used as F (Bernasconi, Codenotti, and Simon 1996), but we also consider two recently introduced FTs (FT3, FT4) due to their information-theoretic interpretation given in Püschel and Wendler (2020):

$$\text{FT3: } F_{y,x} = (-1)^{|x|} \mathbb{I}_{\min(x,y)=x}, \quad (5)$$

$$\text{FT4: } F_{y,x} = (-1)^{|\min(x,y)|} \mathbb{I}_{\max(x,y)=1_m}, \quad (6)$$

$$\text{WHT: } F_{y,x} = \frac{1}{2^m} (-1)^{|\min(x,y)|}. \quad (7)$$

Here, \min is the elementwise minimum (intersection of sets), \max analogous, $|\cdot|$ is the set size, 1_m denotes the m -dimensional vector of 1s, and the indicator function \mathbb{I}_P is equal to 1 if the predicate P is true and 0 otherwise.

Notions of Fourier-sparsity. The notion of Fourier-sparsity has gained considerable attention in recent years, leading to highly efficient algorithms to compute FTs (Stobbe and Krause 2012; Amrollahi et al. 2019; Anonymous 2020). Further, many important classes of set functions are

known to be Fourier-sparse including (hyper)graph cuts, hypergraph valuations, and decision trees (Abraham et al. 2012) and can thus be learned efficiently. The benefit of considering multiple FTs is that they offer different, non-equivalent notions of sparsity.

Example and interpretation. Consider the set of items $M := \{1, 2, 3\}$ and the associated reported value function \hat{v}_i shown below (where we use 001 as a shorthand notation for $(0, 0, 1)$), together with the corresponding FCs $\phi_{\hat{v}_i}$:

	000	100	010	001	110	101	011	111
\hat{v}_i	0	1	1	1	3	3	3	5
FT3	0	-1	-1	-1	1	1	1	1
FT4	5	-2	-2	-2	0	0	0	1
WHT	17/8	-7/8	-7/8	-7/8	1/8	1/8	1/8	1/8

This bidder exhibits complementary effects for each bundle containing more than one item, as can be seen, e.g., from $3 = \hat{v}_i(110) > \hat{v}_i(100) + \hat{v}_i(010) = 2$ and $5 = \hat{v}_i(111) > \hat{v}_i(100) + \hat{v}_i(010) + \hat{v}_i(001) = 3$. Observe that while this value function is sparse in FT4, i.e., $\phi_{\hat{v}_i}(110) = \phi_{\hat{v}_i}(101) = \phi_{\hat{v}_i}(011) = 0$, it is neither sparse in FT3 nor WHT. Note that the coefficients $\phi_{\hat{v}_i}(100)$, $\phi_{\hat{v}_i}(010)$, and $\phi_{\hat{v}_i}(001)$ capture the value of single items and thus cannot be zero.

Fourier-sparse approximations. In practice, \hat{v}_i may only be approximately sparse. However, it may still be approximated well by a small, carefully chosen subset of coefficients. Formally, if $\mathcal{S}_i \subseteq \text{supp}(\phi_{\hat{v}_i})$ with $|\mathcal{S}_i| = k$, we call

$$\tilde{v}_i(x) := \sum_{y \in \mathcal{S}_i} F_{x,y}^{-1} \phi_{\hat{v}_i}(y) \text{ for all } x \in \mathcal{X} \quad (8)$$

a k -Fourier-sparse approximation of \hat{v}_i . We denote the corresponding vector of FCs by $\phi_{\tilde{v}_i|_{\mathcal{S}_i}} := (\phi_{\tilde{v}_i}(y))_{y \in \mathcal{S}_i}$.

4 Fourier Transform-based WDPs

To leverage Fourier analysis for auction design, we represent bidders' reported value functions using Fourier-sparse approximations. An important step in most auction designs is to find the social welfare-maximizing allocation given bidder's reports, which is known as the *Winner Determination Problem* (WDP). Thus, to apply FT in such mechanisms, we need to be able to solve the WDP efficiently. Accordingly, we next derive MIP formulations for each of the FTs.

For each bidder $i \in N$ let $\tilde{v}_i : \mathcal{X} \rightarrow \mathbb{R}_+$ be the Fourier-sparse approximation of the bidder's reported value function \hat{v}_i . Next, we define the *Fourier transform-based WDP*.

Definition 1. (FOURIER TRANSFORM-BASED WDP)

$$\text{argmax}_{a \in \mathcal{F}} \sum_{i \in N} \tilde{v}_i(a_i). \quad (\text{FT-WDP})$$

For all $x, y \in \mathbb{R}^d$, let $x \leq y$, $\max(x, y)$ and $(-1)^x$ be defined componentwise, and let $\langle \cdot, \cdot \rangle$ denote the Euclidean scalar product. First, we formulate succinct representations of \tilde{v}_i for all considered FTs.

Lemma 1. (SUCCINCT REPRESENTATIONS) *For $i \in N$ let $\mathcal{S}_i = \{y^{(1)}, \dots, y^{(k)}\}$ be the support of a k -Fourier-sparse approximation \tilde{v}_i and let $W_i \in \{0, 1\}^{k \times m}$ be defined as:*

$$(W_i)_{l,j} := \begin{cases} 1 & \text{if } y_j^{(l)} = 1, \\ 0 & \text{otherwise.} \end{cases} \quad (9)$$

Then \tilde{v}_i can be rewritten for the different FTs as

$$\text{FT3: } \tilde{v}_i(x) = \langle \phi_{\tilde{v}_i|_{\mathcal{S}_i}}, \max(0_k, 1_k - W_i(1_m - x)) \rangle \quad (10)$$

$$\text{FT4: } \tilde{v}_i(x) = \langle \phi_{\tilde{v}_i|_{\mathcal{S}_i}}, \max(0_k, 1_k - W_i x) \rangle \quad (11)$$

$$\text{WHT: } \tilde{v}_i(x) = \langle \phi_{\tilde{v}_i|_{\mathcal{S}_i}}, (-1)^{W_i x} \rangle. \quad (12)$$

The proof of Lemma 1 follows by rewriting the respective FTs from Püschel and Wendler (2020) using indicator notation. Please see the technical appendix Section B.1 for the details. Using Lemma 1 and rewriting $\max(\cdot, \cdot)$ and $(-1)^\cdot$ as linear constraints, we can formulate (FT-WDP) as a MIP.

Theorem 1. (FOURIER TRANSFORM-BASED MIPS) *Let $\tilde{v}_i : \mathcal{X} \rightarrow \mathbb{R}$ be a k -Fourier-sparse approximation as defined in (10), (11), or (12). Then there exists a constant $C > 0$ such that the MIP defined by the following objective*

$$\text{argmax}_{a \in \mathcal{F}, \beta_i \in \{0,1\}^k} \sum_{i \in N} \langle \phi_{\tilde{v}_i|_{\mathcal{S}_i}}, \alpha_i \rangle, \quad (13)$$

and for $i \in N$ one set of transform specific constraints (14)–(16), or (17)–(19), or (20)–(22), is equivalent to (FT-WDP).

$$\text{FT3: } \text{s.t. } \alpha_i \geq 1_k - W_i(1_m - a_i) \quad (14)$$

$$\alpha_i \leq 1_k - W_i(1_m - a_i) + C\beta_i \quad (15)$$

$$0_k \leq \alpha_i \leq C(1_k - \beta_i) \quad (16)$$

$$\text{FT4: } \text{s.t. } \alpha_i \geq 1_k - W_i a_i \quad (17)$$

$$\alpha_i \leq 1_k - W_i a_i + C\beta_i \quad (18)$$

$$0_k \leq \alpha_i \leq C(1_k - \beta_i) \quad (19)$$

$$\text{WHT: } \text{s.t. } \alpha_i = -2\beta_i + 1_k \quad (20)$$

$$\beta_i = W_i a_i - 2\gamma_i \quad (21)$$

$$\gamma_i \in \mathbb{Z}^k \quad (22)$$

Please see the technical appendix Section B.2 for a proof of Theorem 1. Using Theorem 1, we can solve (FT-WDP) for all FTs using standard MIP-solvers like CPLEX.¹

5 Analyzing the Potential of a FT-based CA

In this section, we experimentally evaluate the FTs and propose an FT-based allocation rule that motivates our practical hybrid ICA mechanism presented later in Section 6.

For our experiments, we use the spectrum auction test suite (SATS) version 0.6.4 (Weiss, Lubin, and Seuken 2017). SATS enables us to generate synthetic CA instances in different domains. Furthermore, we have access to each bidder's *true* full value function v_i as well as the efficient allocation $a^* \in \mathcal{F}$. When simulating bidders in our experiments, we assume straightforward truthful bidding (i.e., $\tilde{v}_i = v_i$, for all $i \in N$). We consider three domains:

The Global Synergy Value Model (GSVM) (Goeree and Holt 2010) has 18 items, 6 *regional* and 1 *national bidder*.

The Local Synergy Value Model (LSVM) (Scheffel, Ziegler, and Bichler 2012) consists of 5 *regional bidders*, 1 *national bidder* and 18 items. Complementarities arise from spatial proximity of items.

The Multi-Region Value Model (MRVM) (Weiss, Lubin, and Seuken 2017) consists of 98 items and 10 bidders, categorized as *national*, *regional*, or *local*. It models large US and Canadian spectrum auctions.

¹In our experiments we use CPLEX 12.10.0.0.

Domain	k	Bidder	FT3	FT4	WHT	NN
GSVM	50	Nat.	37.8 \pm 1.7	43.7 \pm 1.8	4.3 \pm 0.2	14.7 \pm 0.9
		Reg.	18.7 \pm 1.6	29.7 \pm 2.2	3.8 \pm 0.3	10.8 \pm 2.0
	100	Nat.	11.3 \pm 0.7	14.2 \pm 0.8	1.8 \pm 0.1	9.0 \pm 1.8
		Reg.	0.0 \pm 0.0	1.4 \pm 0.2	0.4 \pm 0.1	7.2 \pm 0.9
	200	Nat.	0.0 \pm 0.0	0.0 \pm 0.0	0.0 \pm 0.0	5.7 \pm 0.4
		Reg.	0.0 \pm 0.0	0.0 \pm 0.0	0.0 \pm 0.0	5.2 \pm 0.8
LSVM	50	Nat.	74.7 \pm 0.9	342.6 \pm 5.1	36.6 \pm 0.5	67.6 \pm 2.1
		Reg.	27.3 \pm 1.8	48.7 \pm 2.2	9.2 \pm 0.4	22.6 \pm 1.2
	100	Nat.	78.4 \pm 1.0	580.2 \pm 7.9	31.2 \pm 0.4	48.7 \pm 1.2
		Reg.	28.2 \pm 2.3	48.5 \pm 2.7	6.8 \pm 0.3	17.8 \pm 0.7
	200	Nat.	95.8 \pm 1.2	639.0 \pm 10.0	26.2 \pm 0.3	40.6 \pm 0.7
		Reg.	25.8 \pm 2.0	43.1 \pm 2.4	5.3 \pm 0.3	15.3 \pm 0.9

Table 1: Reconstruction error of k -Fourier sparse approximations \tilde{v}_i and NNs trained on k randomly selected bundles. Winner models are colored in blue.²

5.1 Reconstruction Error of Fourier Transforms

We first validate the FT approach by comparing the reconstruction error of the FTs in the medium-sized domains GSVM and LSVM, where we can still compute the full FT (in contrast to MRVM). For now, we assume that we have access to bidders’ full reported value functions. In Procedure 1, we determine the best k -Fourier-sparse approximation \tilde{v}_i .

Procedure 1. (BEST FCs GIVEN FULL ACCESS TO \hat{v}_i)
Compute all FCs by using the full FT for each bidders’ reported value function $\phi_{\tilde{v}_i} = F\hat{v}_i$. Next, determine the k best FCs $\phi_{\tilde{v}_i|S_i}$ in terms of quadratic error $\|\hat{v}_i - \tilde{v}_i\|_2^2$ as follows:
*i. **WHT:** use the FCs with the k largest absolute values.*
*ii. **FT3 and FT4:** use the FCs with the k largest coefficients $|\phi_{\tilde{v}_i}(y)|\|F_{\cdot,y}^{-1}\|_2$, where $F_{\cdot,y}^{-1}$ denotes the y^{th} column.*

We provide details for *i.* and *ii.* in the technical appendix Section C. Using \tilde{v}_i , we then calculate the reconstruction RMSE $(\frac{1}{2^m} \sum_{x \in \mathcal{X}} (\hat{v}_i(x) - \tilde{v}_i(x))^2)^{1/2}$ averaged over 100 instances and bidders of the same type. In Table 1, we present the RMSEs with a 95%-confidence interval for the three FTs. Furthermore, we present the RMSE for NNs, where we used the same architectures as reported in Weissteiner and Seuken (2020) and trained them on k random bundle-value pairs.

For GSVM, we observe that we can perfectly reconstruct \hat{v}_i with the 200 best FCs, which shows that GSVM is 200-sparse. In contrast, LSVM is non-sparse, and we do not achieve perfect reconstruction with 200 FCs. Overall, we observe that the WHT outperforms FT3 and FT4. Moreover, we see that, if we could compute the k best FCs of the WHT from k training points, the WHT would outperform the NNs. However, when designing a practical ICA we do not have access to full value functions. Instead, we must use an algorithm that computes the best FCs using queries.

5.2 A Fourier Transform-based Allocation Rule

We now present a first simple FT-based allocation rule using the *robust sparse WHT algorithm (RWHT)* by Amrollahi

²Note, due to the difference in training methodology, the NN results in Table 1 are only meant as a reference point.

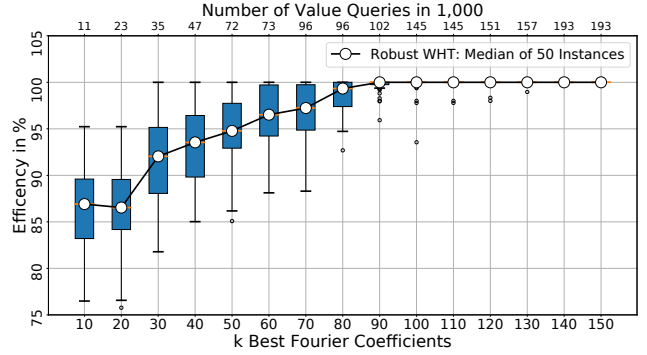


Figure 1: Efficiency of Procedure 2 in GSVM.

et al. (2019) and evaluate its efficiency in GSVM. RWHT learns a Fourier-sparse approximation \tilde{v}_i of \hat{v}_i from queries. We use Procedure 2 to determine an allocation \tilde{a} .

Procedure 2. (WHT-BASED ALLOCATION RULE)

- i. **Estimation:** For each bidder i , compute a k -Fourier-sparse approximation \tilde{v}_i from queries using RWHT.*
- ii. **Optimization:** Solve $\tilde{a} \in \arg\max_{a \in \mathcal{F}} \sum_{i \in N} \tilde{v}_i(a_i)$ by Theorem 1.*

In Figure 1, we present the efficiency of \tilde{a} on 50 GSVM instances for various values of k . We observe that RWHT achieves a median efficiency of 100% when using 90 or more FCs. Nevertheless, the main practical issue with this approach is the number of value queries required (printed on the top of Figure 1). As we can see, RWHT needs 102,000 value queries (around 39% of all bundles) to find the 90 best FCs. For a practical ICA mechanism this is far too many.

6 A Practical Hybrid ICA Mechanism

In this section, we introduce and experimentally evaluate a practical hybrid ICA mechanism, based on FTs and NNs.

6.1 The Hybrid ICA Mechanism

The main issue of the FT-based allocation rule in Section 5.2 is the large number of queries, which we now address.

The key idea is the following: instead of directly applying a sparse FT algorithm (like RWHT) to reported value functions, we apply it to a NN-based (learned) representation. In this way, we evaluate NNs instead of querying the bidders. Based on the FCs of the NNs, we determine a Fourier-sparse approximation \tilde{v}_i using only *few value queries*, where the idea is that the FCs of each NN concentrate on the most dominant FCs of its corresponding value function.

We first present an overview of our hybrid ICA mechanism, leaving the details of individual sub-procedures to Section 6.2.

HYBRID ICA (see Algorithm 3) consists of four phases: (1) the *initialization phase*, (2) the *MLCA phase*, (3) the *Fourier reconstruction phase*, and (4) the *Fourier allocation phase*. It is parameterized by an FT F and the numbers $\ell_1, \ell_2, \ell_3, \ell_4$ of different value queries. In total, HYBRID ICA asks each bidder ℓ_1 random initial queries, ℓ_2 MLCA

Algorithm 3: HYBRID ICA

Params: F Fourier transform; $\ell_1, \ell_2, \ell_3, \ell_4$ query split

- 1 Set $Q^{\text{init}} := \ell_1$ ▷ Initialization phase
- 2 Set $Q^{\text{max}} := \ell_1 + \ell_2$ ▷ MLCA phase
- 3 Run MLCA($Q^{\text{init}}, Q^{\text{max}}$) and elicit ℓ_2 reports R
- 4 **foreach** bidder $i \in N$ **do** ▷ Fourier Reconstr. phase
- 5 Fit NN \mathcal{N}_i to R_i ▷ Learn NN-based representation
- 6 Determine the best FCs of \mathcal{N}_i ▷ (Proc. 3)
- 7 Determine ℓ_3 reconstruction queries \tilde{S}_i ▷ (Proc. 4)
- 8 Ask \tilde{S}_i and add reports to R_i ▷ Four. recon. queries
- 9 Fit Fourier-sparse approximation \tilde{v}_i to R_i ▷ (Proc. 5)
- 10 **end**
- 11 **for** $l = 1, \dots, \ell_4$ **do** ▷ Fourier alloc. phase (Proc. 6)
- 12 Solve $q \in \arg\max_{a \in \mathcal{F}} \sum_{i \in N} \tilde{v}_i(a_i)$ (FT-WDP)
- 13 **foreach** bidder $i \in N$ **do**
- 14 **if** $q_i \in R_i$ **then** ▷ Bundle already queried
- 15 Define $\mathcal{F}' := \{a \in \mathcal{F} : a_i \neq x, \forall x \in R_i\}$
- 16 Resolve $q' \in \arg\max_{a \in \mathcal{F}'} \sum_{i \in N} \tilde{v}_i(a_i)$
- 17 Update $q_i = q'_i$
- 18 **end**
- 19 Query bidder i 's value for q_i and add report to R_i
- 20 Fit Fourier-sparse approx. \tilde{v}_i to R_i ▷ (Proc. 5)
- 21 **end**
- 22 **end**
- 23 Given elicited reports R compute allocation: a_R^* as in (2)
- 24 Given elicited reports R compute VCG payments p
- 25 **return** final allocation a_R^* and VCG payments p

allocation queries, ℓ_3 Fourier reconstruction queries, and ℓ_4 Fourier allocation queries ($= \ell_1 + \ell_2 + \ell_3 + \ell_4$ queries).

In the *initialization phase*, we generate ℓ_1 random initial bundle-value pairs (Line 1). Next, in the *MLCA phase*, we run MLCA using these initial bundles and elicit ℓ_2 MLCA allocation queries (Lines 2–3). In Line 5, we fit for each bidder a NN \mathcal{N}_i on the reports R_i . We incorporate MLCA here, so that the NNs are trained on “meaningfully” elicited reports R_i , rather than just on the ℓ_1 random initial queries. In the *Fourier reconstruction phase*, we compute a Fourier-sparse approximation \tilde{v}_i . Here, we first compute the best FCs of the fitted NNs (Line 6, **Procedure 3**). Then, based on the FCs, we determine ℓ_3 Fourier reconstruction queries $\tilde{S}_i \subseteq \mathcal{X}$ (Lines 7, **Procedure 4**), which we then send to the bidders to receive reports (Line 8). Finally, we fit \tilde{v}_i to the reports R_i received so far (Line 9, **Procedure 5**).

In the last phase, the *Fourier allocation phase*, we use the fitted Fourier-sparse approximations \tilde{v}_i to generate ℓ_4 Fourier allocation queries (**Procedure 6**). Here, we solve the FT-based WDP (Line 12) to determine a candidate q of value queries, ensure in Lines 14–18 that all queries are new, and add the received reports to R_i (Line 19).

Finally, based on all reports R , HYBRID ICA outputs an allocation a_R^* that maximizes the *reported social welfare* and VCG payments p (see the technical appendix Section A.1).

6.2 Fourier Transform-based Procedures

We now present the FT-based procedures of *Hybrid ICA* (for details see the technical appendix Section D.1.).

In Line 6, we use Procedure 3 to compute best FCs of the NN-based representations.

Procedure 3. (BEST FCs OF NEURAL NETWORKS)

- i. If $m \leq 29$: calculate the full FT of the NNs and select the best FCs via Procedure 1.
 - ii. If $m > 29$: use sparse FT algorithms, i.e., RWHT for WHT and SSFT (Anonymous 2020) for FT3 and FT4 to obtain the best FCs of the NNs.³
-

In Line 7, we call Procedure 4 to determine ℓ_3 Fourier reconstruction queries based on the best FCs of the NNs.

Procedure 4. (FOURIER RECONSTRUCTION QUERIES)

- i. **FT3 and FT4:** use the sampling theorems by Püschel and Wendler (2020) to determine queries for the bidders, i.e., bundles $\tilde{S}_i \subseteq \mathcal{X}$, that enable a reconstruction of \tilde{v}_i .
 - ii. **WHT:** use the same queries as for FT4.⁴
-

We use Procedure 5 to fit the FCs $\phi_{\tilde{v}_i|S_i}$ of the Fourier-sparse approximation \tilde{v}_i to received reports R_i (Line 9).

Procedure 5. (FIT FOURIER-SPARSE \tilde{v}_i TO REPORTS)

- i. **FT3 and FT4:** solve the least squares problem defined by the best FCs and reports R_i .
 - ii. **WHT:** use the compressive sensing method by Stobbe and Krause (2012) defined by the best FCs and reports R_i .
-

Procedure 6 generates ℓ_4 Fourier allocation queries.

Procedure 6. (FOURIER ALLOCATION QUERY)

- i. Given fitted \tilde{v}_i , use the MIPs from Theorem 1 to determine a candidate allocation q (Line 12).
 - ii. Optionally, solve another, more restricted, FT-based WDP to ensure that the queries q_i are new (Lines 14–18).
-

6.3 Experiments

We now evaluate the efficiency of our HYBRID ICA and compare it against MLCA in GSVM, LSVM, and MRVM.

Hyperparameter optimization. For both HYBRID ICA and MLCA, we use the same NN architectures as reported in Weissteiner and Seuken (2020) and set the same total query budget of 100 (GSVM and LSVM), and 500 (MRVM). For HYBRID ICA, we performed a hyperparameter optimization on a training set of 100 (GSVM and LSVM)

³If $m > 29$ calculating a full FT is computationally not feasible.

⁴We use this approach, since for the WHT no sampling theorem exists, and the WHT can be decomposed into a triangular matrix and FT4.

NNs Architecture		FT	ℓ_1	ℓ_2	ℓ_3	ℓ_4
GSVM	R:[32, 32] N:[10, 10]	WHT	30	21	20	29
LSVM	R:[32, 32] N:[10, 10, 10]	WHT	30	30	10	30
MRVM	L,R,N:[16, 16]	FT4	30	220	100	150

Table 2: Best configuration of HYBRID ICA.

Mechanism	GSVM (sparse)					LSVM (non-sparse)					MRVM (non-sparse national bidders)					
	Efficiency in %	Reg. in %	Nat. in %	Rev. in %	hrs/ Inst.	Efficiency in %	Reg. in %	Nat. in %	Rev. in %	hrs/ Inst.	Efficiency in %	Lo. in %	Reg. in %	Nat. in %	Rev. in %	hrs/ Inst.
HYBRID ICA	99.59 \pm 0.15	94.34	5.35	80	0.77	98.47 \pm 0.44	88.84	9.62	77	1.89	95.72 \pm 0.43	0.01	1.53	94.18	37	16.28
MLCA	99.17 \pm 0.37	98.11	1.06	79	4.65	99.14 \pm 0.42	93.40	5.75	77	6.09	95.32 \pm 0.32	0.00	0.53	94.79	41	43.26
MLCA+RANDOM	98.16 \pm 0.50	97.47	0.69	75	0.71	97.75 \pm 0.63	92.78	5.27	72	1.86	93.91 \pm 0.36	0.01	0.42	93.48	42	14.68
<i>Efficient Allocation</i>		94.75	5.25				84.03	15.97				0.00	2.11	97.89		

Table 3: A comparison of HYBRID ICA against MLCA and MLCA+RANDOM. All results are averages over 100 (GSVM and LSVM) and 30 (MRVM) instances. For efficiency we give a 95% confidence interval and color the best mechanisms in blue.

and 30 (MRVM) instances, where we optimized the FTs and tried several query parameters $\ell_1, \ell_2, \ell_3, \ell_4$. Table 2 presents the results of the best found HYBRID ICA configuration for each domain.⁵ We observe that WHT works best for the smaller GSVM and LSVM, and FT4 for MRVM.

Experiment Setup. For each domain, we present efficiency, the distribution of efficiency to bidder types, revenue (calculated as $(\sum_{i \in N} p_i)/V(a^*)$) and compute time in hours per instance. To verify the importance of the ℓ_3 Fourier reconstruction and the ℓ_4 Fourier allocation queries, we also present a third mechanism MLCA+RANDOM. MLCA+RANDOM runs the same parametrization as HYBRID ICA with the only exception, that it uses random queries instead of the $\ell_3 + \ell_4$ Fourier-based queries. Thus, comparing HYBRID ICA and MLCA+RANDOM isolates the effect of the Fourier-based queries.

HYBRID ICA vs. MLCA. We now compare the performance of HYBRID ICA against MLCA, as shown in Table 3.⁶ First, we see that HYBRID ICA matches the efficiency of MLCA in all domains. However, HYBRID ICA has two important advantages. First, it leads to a significant computational speedup ($\times 6$ in GSVM, $\times 3$ in LSVM and MRVM). Second, and most importantly, it distributes the efficiency more evenly across bidder types. This also leads to a distribution that more closely resembles the distribution in the efficient allocation (see *Efficient Allocation*). Intuitively, the Fourier-based queries lead to a better exploration of the bundle space than only using *MLCA allocation queries*.

Importance of Fourier-based queries. A comparison of HYBRID ICA to MLCA+RANDOM reveals that the Fourier-based queries lead to significantly better efficiency. Furthermore, we see that MLCA+RANDOM cannot achieve the more balanced distribution of efficiency to bidder types.

Details for HYBRID ICA. Figure 2 shows detailed efficiency results for GSVM (for LSVM and MRVM see the technical appendix Section D.2). We plot the efficiency of the different phases of HYBRID ICA. Starting with $\ell_1 = 30$ random initial queries (Rand. Init.), HYBRID ICA achieves a mean efficiency of 65%. Next, our algorithm performs three MLCA iterations (MLCA 1–3) to ask $\ell_2 = 21$ *MLCA allocation queries* in total.⁷ After that, for 99 instances, HYBRID ICA found an allocation with an efficiency of at least 90%. However, the remaining Fourier-based queries

still significantly increase (by 1.4%) the average efficiency to 99.59%.

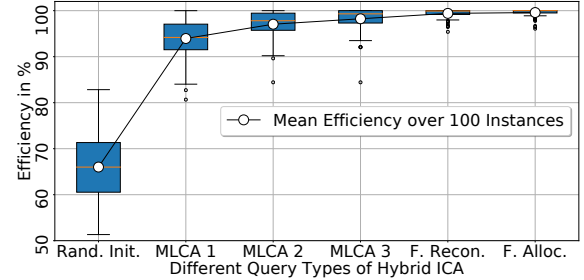


Figure 2: HYBRID ICA in GSVM.

Thus, especially in sparse domains, our Fourier-based approach might be valuable for the design of real-world ICAs. In practice, bidders are often either limited by their cognitive abilities (Scheffel, Ziegler, and Bichler 2012) or use a (low-dimensional) computational model to represent their value function. Thus, it is reasonable to assume that their preferences exhibit only a limited degree of complementarity and complementarity, which is captured well by Fourier-sparsity.

7 Conclusion

In this paper, we have introduced Fourier analysis for the design of combinatorial auctions and laid the foundations for future work in this area. The main idea was to represent bidder’s value functions using Fourier-sparse approximations, providing us with a new lens on bidder’s values in the Fourier domain.

On a technical level, our main contribution was to derive succinct MIPs for the Fourier transform-based WDPs, which makes computing Fourier-based allocation queries practically feasible. We have leveraged this to design a new hybrid ICA mechanism that uses NN-based and Fourier-based queries. Our experiments have shown that our approach matches the economic efficiency of the current benchmark, while achieving a significant computational speedup and a fairer distribution of welfare among bidders.

For future work, it would be interesting to investigate how and why the addition of the Fourier-based queries lead to a fairer distribution of welfare. Furthermore, one could explore the application of our techniques in settings where large amounts of bidding data is available (e.g., in ad auctions), such that the number of queries is no longer a limiting factor for the application of the Fourier analysis framework.

⁵R: $[d_1, d_2, d_3]$ denotes a 3-hidden-layer NN for the regional bidder type with d_1, d_2 and d_3 hidden nodes, respectively.

⁶All results are obtained on a test set of new CA instances.

⁷Recall that *MLCA* asks each bidder n queries per iteration.

8 Acknowledgments

This paper is part of a project that has received funding from the European Research Council (ERC) under the European Unions Horizon 2020 research and innovation programme (Grant agreement No. 805542).

References

- Abraham, I.; Babaioff, M.; Dughmi, S.; and Roughgarden, T. 2012. Combinatorial auctions with restricted complements. In *Proceedings of the 13th ACM Conference on Electronic Commerce*, 3–16.
- Amrollahi, A.; Zandieh, A.; Kapralov, M.; and Krause, A. 2019. Efficiently learning Fourier sparse set functions. In *Advances in Neural Information Processing Systems*, 15120–15129.
- Anonymous, f. p. r. 2020. Learning Set Functions that are Sparse in Non-Orthogonal Fourier Bases. In *Submitted for publication*.
- Ausubel, L.; and Cramton, P. 2011. Auction design for wind rights. *Report to Bureau of Ocean Energy Management, Regulation and Enforcement*.
- Ausubel, L. M.; and Baranov, O. 2017. A practical guide to the combinatorial clock auction. *Economic Journal* 127(605): F334–F350.
- Ausubel, L. M.; Cramton, P.; and Milgrom, P. 2006. The clock-proxy auction: A practical combinatorial auction design. In Cramton, P.; Shoham, Y.; and Steinberg, R., eds., *Combinatorial Auctions*, 115–138. MIT Press.
- Bernasconi, A.; Codenotti, B.; and Simon, J. 1996. On the Fourier analysis of Boolean functions. *preprint* 1–24.
- Blum, A.; Jackson, J.; Sandholm, T.; and Zinkevich, M. 2004. Preference elicitation and query learning. *Journal of Machine Learning Research* 5: 649–667.
- Brero, G.; Lahaie, S.; and Seuken, S. 2019. Fast Iterative Combinatorial Auctions via Bayesian Learning. In *Proceedings of the Thirty-third AAAI Conference of Artificial Intelligence*.
- Brero, G.; Lubin, B.; and Seuken, S. 2017. Probably approximately efficient combinatorial auctions via machine learning. In *Thirty-First AAAI Conference on Artificial Intelligence*.
- Brero, G.; Lubin, B.; and Seuken, S. 2018. Combinatorial Auctions via Machine Learning-based Preference Elicitation. In *Proceedings of the 27th International Joint Conference on Artificial Intelligence and the 23rd European Conference on Artificial Intelligence*.
- Brero, G.; Lubin, B.; and Seuken, S. 2020. Machine Learning-powered Iterative Combinatorial Auctions. *arXiv preprint* <https://arxiv.org/pdf/1911.08042.pdf>.
- Cramton, P. 2013. Spectrum auction design. *Review of Industrial Organization* 42(2): 161–190.
- Dütting, P.; Feng, Z.; Narasimhan, H.; Parkes, D. C.; and Ravindranath, S. S. 2019. Optimal auctions through deep learning. In *Proceedings of the 36th International Conference on Machine Learning*.
- Goeree, J. K.; and Holt, C. A. 2010. Hierarchical package bidding: A paper & pencil combinatorial auction. *Games and Economic Behavior* 70(1): 146–169.
- Lahaie, S. M.; and Parkes, D. C. 2004. Applying learning algorithms to preference elicitation. In *Proceedings of the 5th ACM Conference on Electronic Commerce*.
- Nisan, N.; and Segal, I. 2006. The communication requirements of efficient allocations and supporting prices. *Journal of Economic Theory* 129(1): 192–224.
- O’Donnell, R. 2014. *Analysis of boolean functions*. Cambridge University Press.
- Püschel, M. 2018. A discrete signal processing framework for set functions. In *Proc. International Conference on Acoustics, Speech and Signal Processing (ICASSP)*, 4359–4363. IEEE.
- Püschel, M.; and Wendler, C. 2020. Discrete Signal Processing with Set Functions. *arXiv preprint arXiv:2001.10290*.
- Rahme, J.; Jelassi, S.; Bruna, J.; and Weinberg, S. M. 2020. A Permutation-Equivariant Neural Network Architecture For Auction Design. *arXiv preprint* <https://arxiv.org/pdf/2003.01497.pdf>.
- Scheffel, T.; Ziegler, G.; and Bichler, M. 2012. On the impact of package selection in combinatorial auctions: an experimental study in the context of spectrum auction design. *Experimental Economics* 15(4): 667–692.
- Scheibler, R.; Haghighatshoar, S.; and Vetterli, M. 2015. A fast Hadamard transform for signals with sublinear sparsity in the transform domain. *IEEE Transactions on Information Theory* 61(4): 2115–2132.
- Stobbe, P.; and Krause, A. 2012. Learning Fourier sparse set functions. In *Artificial Intelligence and Statistics*, 1125–1133.
- Weiss, M.; Lubin, B.; and Seuken, S. 2017. Sats: A universal spectrum auction test suite. In *Proceedings of the 16th Conference on Autonomous Agents and Multi-Agent Systems*.
- Weissteiner, J.; and Seuken, S. 2020. Deep Learning-powered Iterative Combinatorial Auctions. In *Proceedings of the 34th AAAI Conference of Artificial Intelligence*.

Appendix

A Preliminaries

In this section, we provide a recap on how to compute VCG payments from bidder’s reports.

A.1 VCG Payments from Reports

Let $R = (R_1, \dots, R_n)$ denote an elicited set of reported bundle-value pairs from each bidder obtained from MLCA (Algorithm 2) or HYBRID ICA (Algorithm 3) and let $R_{-i} := (R_1, \dots, R_{i-1}, R_{i+1}, \dots, R_n)$. We then calculate the VCG payments $p = (p_1, \dots, p_n) \in \mathbb{R}_+^n$ as follows:

Definition 2. (VCG PAYMENTS FROM REPORTS)

$$p_j := \sum_{i \in N \setminus \{j\}} \hat{v}_i \left((a_{R_{-j}}^*)_i \right) - \sum_{i \in N \setminus \{j\}} \hat{v}_i \left((a_R^*)_i \right). \quad (23)$$

where $a_{R_{-i}}^*$ maximizes the reported social welfare when excluding bidder i , i.e.,

$$a_{R_{-j}}^* \in \operatorname{argmax}_{a \in \mathcal{F}} \widehat{V}(a|R_{-j}) = \operatorname{argmax}_{a \in \mathcal{F}} \sum_{\substack{i \in N \setminus \{j\}: \\ (a_i, \hat{v}_i(a_i)) \in R_i}} \hat{v}_i(a_i), \quad (24)$$

and a_R^* is a reported-social-welfare-maximizing allocation (including all bidders), i.e.,

$$a_R^* \in \operatorname{argmax}_{a \in \mathcal{F}} \widehat{V}(a|R) = \operatorname{argmax}_{a \in \mathcal{F}} \sum_{i \in N: (a_i, \hat{v}_i(a_i)) \in R_i} \hat{v}_i(a_i). \quad (25)$$

As argued in Brero, Lubin, and Seuken (2020), using such payments are key for MLCA to induce “good” incentives for bidders to report truthfully. As their incentive analysis also applies to HYBRID ICA, we use them in our design too.

B Fourier Transform-based WDPs

In this Section, we present the proofs of Lemma 1 and Theorem 1.

Let 1_d and 0_d for $d \in \mathbb{N}$ denote the d -dimensional vector of ones and zeros, respectively. For all $x, y \in \mathbb{R}^d$, let $x \leq y$, $\max(x, y)$, $\min(x, y)$ and $(-1)^x$ be defined component-wise, and let $\langle \cdot, \cdot \rangle$ denote the Euclidean scalar product.

We consider the matrix representation F and F^{-1} of the considered FTs from Püschel and Wendler (2020) given by:

$$\mathbf{FT3}: F_{y,x} = (-1)^{|x|} \mathbb{I}_{\min(x,y)=x}, \quad (26)$$

$$F_{x,y}^{-1} = (-1)^{|y|} \mathbb{I}_{\min(x,y)=y}, \quad (27)$$

$$\mathbf{FT4}: F_{y,x} = (-1)^{|\min(x,y)|} \mathbb{I}_{\max(x,y)=1_m}, \quad (28)$$

$$F_{x,y}^{-1} = \mathbb{I}_{\min(x,y)=0_m}, \quad (29)$$

$$\mathbf{WHT}: F_{y,x} = \frac{1}{2^m} (-1)^{|\min(x,y)|}, \quad (30)$$

$$F_{x,y}^{-1} = (-1)^{|\min(x,y)|}. \quad (31)$$

The Fourier-sparse approximations used in the WDPs are defined in terms of F^{-1} .

B.1 Proof of Lemma 1

Lemma 2. (SUCCINCT REPRESENTATIONS) *For $i \in N$ let $\mathcal{S}_i = \{y^{(1)}, \dots, y^{(k)}\}$ be the support of a k -Fourier-sparse approximation \tilde{v}_i and let $W_i \in \{0, 1\}^{k \times m}$ be defined as:*

$$(W_i)_{l,j} := \begin{cases} 1 & \text{if } y_j^{(l)} = 1, \\ 0 & \text{otherwise.} \end{cases} \quad (32)$$

Then \tilde{v}_i can be rewritten for the different FTs as

$$\mathbf{FT3}: \tilde{v}_i(x) = \langle \phi_{\tilde{v}_i|_{\mathcal{S}_i}}, \max(0_k, 1_k - W_i(1_m - x)) \rangle \quad (33)$$

$$\mathbf{FT4}: \tilde{v}_i(x) = \langle \phi_{\tilde{v}_i|_{\mathcal{S}_i}}, \max(0_k, 1_k - W_i x) \rangle \quad (34)$$

$$\mathbf{WHT}: \tilde{v}_i(x) = \langle \phi_{\tilde{v}_i|_{\mathcal{S}_i}}, (-1)^{W_i x} \rangle. \quad (35)$$

Proof. In this proof we are going to make use of the equivalence between bundles (= indicator vectors) and sets. Recall that $x, y \in \mathcal{X} = \{0, 1\}^m$ are bundles and bundles correspond to subsets of items. We can translate set operations such as intersection, union and complement to indicator vectors as follows:

$$x \cap y = \min(x, y), \quad (36)$$

$$x \cup y = \max(x, y), \quad (37)$$

$$(x)^c = 1_m - x, \quad (38)$$

where we slightly abused notation by identifying the indicator vectors with their corresponding subsets on the left hand sides of (36)–(38). Furthermore, it holds that:

$$|\min(x, y)| = y^T x = \sum_{i=1}^m x_i y_i \quad (39)$$

FT3. Let F denote the matrix representation of FT3 in (5). Here, we slightly adjust the Fourier basis to our needs by flipping the signs of the negative basis vectors, i.e., negative columns $(F_{\cdot, y}^{-1})$ with $|y|$ odd in F^{-1} . This way we obtain $\tilde{F}_{x,y}^{-1} = \mathbb{I}_{\min(x,y)=y}$. We do so because it does not change the basis (when computing the corresponding Fourier transform the signs of respective Fourier coefficients flip) and it makes the implementation of FT3 more similar to the one of FT4. After changing the signs of the basis vectors in described manner, we have

$$\tilde{v}_i(x) = \sum_{y \in \mathcal{S}_i} \tilde{F}_{x,y}^{-1} \phi_{\tilde{v}_i}(y) \quad (40)$$

$$= \sum_{y \in \mathcal{S}_i} \mathbb{I}_{\min(1_m - x, y) = 0_m} \phi_{\tilde{v}_i}(y) \quad (41)$$

$$= \langle (\mathbb{I}_{\min(1_m - x, y) = 0_m})_{y \in \mathcal{S}_i}, \phi_{\tilde{v}_i|_{\mathcal{S}_i}} \rangle, \quad (42)$$

where we used $x \cap y = y \Leftrightarrow x^c \cap y = \emptyset$. Now, the claim follows by observing that

$$\mathbb{I}_{\min(1_m - x, y) = 0_m} = \max(0, 1 - y^T(1_m - x)), \quad (43)$$

which is a direct consequence of $|\min(1_m - x, y)| = y^T(1_m - x)$, and recalling that for each $y \in \mathcal{S}_i$ there is a respective row y^T in W_i .

FT4. Let F be the matrix representation of FT4 in (6). By definition, we have

$$\tilde{v}_i(x) = \sum_{y \in \mathcal{S}_i} F_{x,y}^{-1} \phi_{\tilde{v}_i}(y) \quad (44)$$

$$= \sum_{y \in \mathcal{S}_i} \mathbb{I}_{\min(x, y) = 0_m} \phi_{\tilde{v}_i}(y) \quad (45)$$

$$= \langle (\mathbb{I}_{\min(x, y) = 0_m})_{y \in \mathcal{S}_i}, \phi_{\tilde{v}_i|_{\mathcal{S}_i}} \rangle. \quad (46)$$

Now, the claim follows by observing that

$$\mathbb{I}_{\min(x, y) = 0_m} = \max(0, 1 - y^T x), \quad (47)$$

which is a direct consequence of $|\min(x, y)| = y^T x$, and recalling that for each $y \in \mathcal{S}_i$ there is a respective row y^T in

W_i .

WHT. Let F be the matrix representation of WHT in (7). By definition, we have

$$\tilde{v}_i(x) = \sum_{y \in \mathcal{S}_i} F_{x,y}^{-1} \phi_{\tilde{v}_i}(y) \quad (48)$$

$$= \sum_{y \in \mathcal{S}_i} (-1)^{y^T x} \phi_{\tilde{v}_i}(y) \quad (49)$$

$$= \langle ((-1)^{y^T x})_{y \in \mathcal{S}_i}, \phi_{\tilde{v}_i|_{\mathcal{S}_i}} \rangle. \quad (50)$$

Now, the claim follows by recalling that for each $y \in \mathcal{S}_i$ there is a respective row y^T in W_i . \square

B.2 Proof of Theorem 1

We first state and proof two elementary lemmata.

For $x \in \mathbb{R}^d$ let $x \pmod{2}$ be defined component-wise.

Lemma 3. (MAX REPRESENTATION) *Let $\zeta, \eta \in \mathbb{R}^d$ for $d \in \mathbb{N}$ and $C > 0$ such that for all $l \in \{1, \dots, d\}$ it holds that $|\zeta_l - \eta_l| \leq C$. Let $\alpha := \max(\zeta, \eta)$ and consider the polytope \mathcal{P} in $(\tilde{\alpha}, \beta)$ defined by (51)–(55)*

$$\tilde{\alpha} \geq \eta \quad (51)$$

$$\tilde{\alpha} \leq \eta + C\beta \quad (52)$$

$$\tilde{\alpha} \geq \zeta \quad (53)$$

$$\tilde{\alpha} \leq \zeta + C(1_d - \beta) \quad (54)$$

$$\beta \in \{0, 1\}^d. \quad (55)$$

Then it holds that $\mathcal{P} \neq \emptyset$ and every element $(\tilde{\alpha}, \beta) \in \mathcal{P}$ satisfies $\tilde{\alpha} = \alpha$.

Proof. Non-emptiness follows from the assumption that $|\zeta_l - \eta_l| \leq C$ for all $l \in \{1, \dots, d\}$. For any $l \in \{1, \dots, d\}$ we have to distinguish the following cases:

$$\zeta_l < \eta_l \implies \beta_l = 0, \tilde{\alpha}_l = \eta_l = \max(\zeta_l, \eta_l) = \alpha_l$$

$$\zeta_l > \eta_l \implies \beta_l = 1, \tilde{\alpha}_l = \zeta_l = \max(\zeta_l, \eta_l) = \alpha_l$$

$$\zeta_l = \eta_l \implies \tilde{\alpha}_l = \zeta_l = \eta_l = \max(\zeta_l, \eta_l) = \alpha_l$$

This yields that $\tilde{\alpha} = \alpha$. \square

Lemma 4. (ODD-EVEN REPRESENTATION) *Let $\zeta \in \mathbb{Z}^d$ for $d \in \mathbb{N}$. Let $\beta := \zeta \pmod{2} \in \{0, 1\}^d$ and consider the polytope \mathcal{P} in $(\tilde{\beta}, \gamma)$ defined by (56) and (57)*

$$\tilde{\beta} = \zeta - 2\gamma \quad (56)$$

$$\tilde{\beta} \in \{0, 1\}^d, \gamma \in \mathbb{Z}^d. \quad (57)$$

Then it holds that $\mathcal{P} \neq \emptyset$ and every element $(\tilde{\beta}, \gamma) \in \mathcal{P}$ satisfies $\tilde{\beta} = \beta$.

Proof. Non-emptiness follows since $\zeta \in \mathbb{Z}^d$ per assumption. For any $l \in \{1, \dots, d\}$ we have to distinguish the following cases:

$$\zeta_l \pmod{2} = 0 \implies \gamma_l = \frac{\zeta_l}{2}, \tilde{\beta}_l = 0 = \beta_l$$

$$\zeta_l \pmod{2} = 1 \implies \gamma_l = \frac{\zeta_l - 1}{2}, \tilde{\beta}_l = 1 = \beta_l$$

Thus $\tilde{\beta} = \beta$. \square

For each bidder $i \in N$ let $\tilde{v}_i : \mathcal{X} \rightarrow \mathbb{R}_+$ be the Fourier-sparse approximation of the bidder's reported value function \hat{v}_i . Then the *Fourier transform-based WDP* was defined as follows:

Definition 3. (FOURIER TRANSFORM-BASED WDP)

$$\operatorname{argmax}_{a \in \mathcal{F}} \sum_{i \in N} \tilde{v}_i(a_i). \quad (\text{FT-WDP})$$

Next, we proof Theorem 2.

Theorem 2. (FOURIER TRANSFORM-BASED MIPs) *Let $\tilde{v}_i : \mathcal{X} \rightarrow \mathbb{R}$ be a k -Fourier-sparse approximation as defined in (10), (11), or (12). Then there exists a constant $C > 0$ such that the MIP defined by the following objective*

$$\operatorname{argmax}_{a \in \mathcal{F}, \beta_i \in \{0, 1\}^k} \sum_{i \in N} \langle \phi_{\tilde{v}_i|_{\mathcal{S}_i}}, \alpha_i \rangle, \quad (58)$$

and for $i \in N$ one set of transform specific constraints (59)–(61), or (62)–(64), or (65)–(67), is equivalent to (FT-WDP).

$$\textbf{FT3:} \quad \text{s.t. } \alpha_i \geq 1_k - W_i(1_m - a_i) \quad (59)$$

$$\alpha_i \leq 1_k - W_i(1_m - a_i) + C\beta_i \quad (60)$$

$$0_k \leq \alpha_i \leq C(1_k - \beta_i) \quad (61)$$

$$\textbf{FT4:} \quad \text{s.t. } \alpha_i \geq 1_k - W_i a_i \quad (62)$$

$$\alpha_i \leq 1_k - W_i a_i + C\beta_i \quad (63)$$

$$0_k \leq \alpha_i \leq C(1_k - \beta_i) \quad (64)$$

$$\textbf{WHT:} \quad \text{s.t. } \alpha_i = -2\beta_i + 1_k \quad (65)$$

$$\beta_i = W_i a_i - 2\gamma_i \quad (66)$$

$$\gamma_i \in \mathbb{Z}^k \quad (67)$$

Proof. We proof the equivalence for each of the FTs and corresponding MIPs separately.

- **FT3**

Let $C > 0$ such that $|[1_k - W_i(1_m - a_i)]_l| \leq C$ for all $l \in \{1, \dots, k\}$, $i \in N$, and $a \in \mathcal{F}$. We then define

$$\alpha_i := \max(0_k, 1_k - W_i(1_m - a_i)) \text{ for all } i \in N,$$

and apply for each α_i Lemma 3 to $\zeta := 0_k$ and $\eta := 1_k - W_i(1_m - a_i)$, which concludes the proof for FT3.

- **FT4:**

This follows analogously as for the FT3 when defining $\alpha_i := \max(0_k, 1_k - W_i a_i)$, $\zeta := 0_k$ and $\eta := 1_k - W_i a_i$.

- **WHT:**

Since for all $i \in N$ and $a \in \mathcal{F}$ it holds that $W_i a_i \in \mathbb{Z}^k$, an immediate consequence from Lemma 4 is that $\beta_i = W_i a_i \pmod{2}$ and $(-1)^{W_i a_i} = -2\beta_i + 1_k$, which concludes the proof for the WHT. \square

C Analyzing the Potential of a FT-based CA

Let F denote the corresponding matrix representation of the FT3, FT4, or the WHT. Furthermore, fix bidder $i \in N$ and for $\mathcal{S}_i \subseteq \text{supp}(\phi_{\hat{v}_i})$, $|\mathcal{S}_i| = k \ll 2^m$ let

$$\tilde{v}_i = \sum_{y \in \mathcal{S}_i} F_{x,y}^{-1} \phi_{\hat{v}_i}(y) = F_{\cdot, \mathcal{S}_i}^{-1} \phi_{\hat{v}_i}|_{\mathcal{S}_i}, \quad (68)$$

be a k -Fourier-sparse approximation, where we denote by $F_{\cdot, \mathcal{S}_i}^{-1}$ the sub matrix of F^{-1} obtained by selecting the columns indexed by the bundles in \mathcal{S}_i .

C.1 Best Fourier Coefficients WHT

For the WHT, we consider the following optimization problem of selecting the k -best FCs with respect to the quadratic error:

$$\mathcal{S}_i^* \in \underset{\mathcal{S}_i \subseteq \text{supp}(\phi_{\hat{v}_i}), |\mathcal{S}_i|=k}{\text{argmin}} \|\hat{v}_i - F_{\cdot, \mathcal{S}_i}^{-1} \phi_{\hat{v}_i}|_{\mathcal{S}_i}\|_2^2. \quad (69)$$

Then, it follows that \mathcal{S}_i^* consists out of those bundles $\{y^{(l)}\}_{l=1}^k$ with the largest absolute value of the corresponding FCs $\{\phi_{\hat{v}_i}(y^{(l)})\}_{l=1}^k$. This can be seen as follows.

$$\|\hat{v}_i - F_{\cdot, \mathcal{S}_i}^{-1} \phi_{\hat{v}_i}|_{\mathcal{S}_i}\|_2^2 = \left\| \sum_{y \notin \mathcal{S}_i} F_{\cdot, y}^{-1} \phi_{\hat{v}_i}(y) \right\|_2^2 \quad (70)$$

$$= \sum_{x, y \notin \mathcal{S}_i} \langle F_{\cdot, x}^{-1}, F_{\cdot, y}^{-1} \rangle \phi_{\hat{v}_i}(x) \phi_{\hat{v}_i}(y) \quad (71)$$

$$= \sum_{y \notin \mathcal{S}_i} \phi_{\hat{v}_i}(y)^2, \quad (72)$$

where in the last equality we used that F^{-1} is an orthogonal matrix and thus its columns fulfill $\langle F_{\cdot, x}^{-1}, F_{\cdot, y}^{-1} \rangle = \mathbb{I}_{x=y}$.

C.2 Best Fourier Coefficients FT3 and FT4

For FT3 and FT4, we use the triangular inequality

$$\|\hat{v}_i - F_{\cdot, \mathcal{S}_i}^{-1} \phi_{\hat{v}_i}|_{\mathcal{S}_i}\|_2 \leq \sum_{y \notin \mathcal{S}_i} |\phi_{\hat{v}_i}(y)| \|F_{\cdot, y}^{-1}\|_2$$

to get an upper bound of the quadratic error $\|\hat{v}_i - \tilde{v}_i\|_2^2$ and select the FCs with the k largest coefficients $|\phi_{\hat{v}_i}(y)| \|F_{\cdot, y}^{-1}\|_2$, where $F_{\cdot, y}^{-1}$ denotes the y^{th} column of F^{-1} .

D A Practical Hybrid ICA Mechanism

D.1 Technical Details of HYBRID ICA

In this section we provide the technical details for the implementation of HYBRID ICA. In particular, we explain the Fourier Transform-based procedures: Procedures 3–5.

Determining the best FCs of NN

Procedure 3. (BEST FCs OF NEURAL NETWORKS)

- i. If $m \leq 29$: calculate the full FT of the NNs and select the best FCs.
- ii. If $m > 29$: use sparse FT algorithms, i.e., RWHT for WHT and SSFT (Anonymous 2020) for FT3 and FT4 to obtain the best FCs of the NNs.

Using Procedure 3 we determine the best FCs of the neural network estimates of each bidder. We distinguish the two cases:

- **Small number of items:** if the number of items is small enough, i.e., $m \leq 29$, we determine the best FCs (and associated locations $\mathcal{S}_i \subset \mathcal{X}$) of \mathcal{N}_i for all FTs by computing its full Fourier transform $F\mathcal{N}_i = \phi_{\mathcal{N}_i}$ using the respective algorithms from Püschel and Wendler (2020).
- **Large number of items:** if the number of items is too large, i.e., $m > 29$, we cannot compute the full Fourier transform and thus require sparse FT algorithms to compute the locations of the best FCs. For the WHT, we can do so by using the *robust sparse WHT algorithm (RWHT)* by Amrollahi et al. (2019). For FT3 and FT4, we use the *sparse set function Fourier transform (SSFT)* algorithm by Anonymous (2020). Both algorithms learn the best FCs as well as their support by only using queries from the corresponding set function (= a bidder's value function), and thus do not require a representation of the exponentially large full set function.
- **Best WHT FCs:** for the WHT the best FCs are the ones with the largest absolute values (see Section C.1). We select the locations of the ℓ_3 best NN FCs, i.e., $|\mathcal{S}_i| = \ell_3$. We do so because we are going to use the *compressive sensing method* by Stobbe and Krause (2012), which only requires a superset of the support $\text{supp}(\phi_{\hat{v}_i})$, in **Procedure 5** to fit the Fourier-sparse approximations \tilde{v}_i to the bidders' reports R_i . In our experiments, we set $c = 2$. Ideally, we would like to choose c as large as possible to ensure that the best NN FCs actually overlap with the best FCs of \hat{v}_i , however, there is a trade-off between the number of samples (and also running time) required by the *compressive sensing method* and the size of the support superset. We did not optimize this hyperparameter.
- **Best FT3 and FT4 FCs:** for the FT3 and FT4 we use a heuristic based on the triangular inequality to select the best FCs and their locations (see Section C.2). As neither FT3 nor FT4 are orthogonal or satisfy the restricted isometry property required by the *compressive sensing method*, we only take the best ℓ_3 locations of NN FCs, i.e., $|\mathcal{S}_i| = \ell_3$.

Notice that the goal of **Procedure 3** is solely to determine a set of bundles $\mathcal{S}_i \subseteq \mathcal{X}$ that is likely to contain many of the dominant FCs of \hat{v}_i . This set \mathcal{S}_i is then used to determine reconstructing queries $\tilde{\mathcal{S}}_i$.

Determining reconstruction queries

Procedure 4. (FOURIER RECONSTRUCTION QUERIES)

- i. **FT3 and FT4:** use the sampling theorems by Püschel and Wendler (2020) to determine queries for the bidders, i.e., bundles $\tilde{\mathcal{S}}_i \subseteq \mathcal{X}$, that enable a reconstruction of \tilde{v}_i .
- ii. **WHT:** use the same queries as for FT4.

We make use of the sampling theorems for FT3 and FT4 presented by Püschel and Wendler (2020) to obtain reconstruction queries, i.e., queries that help obtaining a small reconstruction error $\|\hat{v}_i - \tilde{v}_i\|_2$. Our rationale here is that

the queries given by the sampling theorem $\tilde{\mathcal{S}}_i$ would lead to $\|\hat{v}_i - \tilde{v}_i\|_2 = 0$ for $\text{supp}(\phi_{\tilde{v}_i}) = \mathcal{S}_i$. The sampling theorem by Püschel and Wendler (2020) selects rows $\tilde{\mathcal{S}}_i$ such that $F_{\tilde{\mathcal{S}}_i, \mathcal{S}_i}^{-1}$ is of full rank, because then (iff $\text{supp}(\phi_{\tilde{v}_i}) = \mathcal{S}_i$) the Fourier coefficients $\phi_{\tilde{v}_i|_{\mathcal{S}_i}}$ are the solution of the linear system of equations $\hat{v}_{i|\tilde{\mathcal{S}}_i} = F_{\tilde{\mathcal{S}}_i, \mathcal{S}_i}^{-1} \phi_{\tilde{v}_i|_{\mathcal{S}_i}}$. In particular, the theorem yields

- **FT3:** $\tilde{\mathcal{S}}_i = \mathcal{S}_i$,
- **FT4:** $\tilde{\mathcal{S}}_i = \{1_m - y : y \in \mathcal{S}_i\}$.

For the WHT there is no sampling theorem. However, we use

$$\tilde{\mathcal{S}}_i = \{1_m - y : |\phi_{\mathcal{N}_i}(y)| \text{ is in the } \ell_3 \text{ largest in } \mathcal{S}_i\}$$

as a heuristic to obtain reconstruction queries. Choosing $\tilde{\mathcal{S}}_i$ in that way empirically often leads to a full-rank submatrix $F_{\tilde{\mathcal{S}}_i, \mathcal{Z}}^{-1}$ of the inverse WHT obtained by selecting the rows indexed by $\tilde{\mathcal{S}}_i$ and the columns indexed by \mathcal{Z} , where $\mathcal{Z} \subseteq \mathcal{S}_i$ are the locations of the ℓ_3 in absolute value largest FCs in \mathcal{S}_i , i.e., $\mathcal{Z} := \{y : |\phi_{\mathcal{N}_i}(y)| \text{ is in the } \ell_3 \text{ largest in } \mathcal{S}_i\}$. If $F_{\tilde{\mathcal{S}}_i, \mathcal{Z}}^{-1}$ is full rank and $\text{supp}(\phi_{\tilde{v}_i}) = \mathcal{Z}$, the Fourier coefficients $\phi_{\tilde{v}_i|_{\mathcal{Z}}}$ are the solution of the linear system of equations $\hat{v}_{i|\tilde{\mathcal{S}}_i} = F_{\tilde{\mathcal{S}}_i, \mathcal{Z}}^{-1} \phi_{\tilde{v}_i|_{\mathcal{Z}}}$.

Fitting the Fourier-sparse approximations

Procedure 5. (FIT FOURIER-SPARSE \tilde{v}_i TO REPORTS)

- FT3 and FT4:** solve the least squares problem defined by the best FCs and reports R_i .
- WHT:** use the compressive sensing method by Stobbe and Krause (2012) defined by the best FCs and reports R_i .

Lastly, we need to fit our Fourier-sparse approximations \tilde{v}_i with $\text{supp}(\phi_{\tilde{v}_i}) = \mathcal{S}_i$ to the elicited reports $R_i := \{(x^{(l)}, \hat{v}_i(x^{(l)}))\}$. That is, we determine values $w \in \mathbb{R}^{|\mathcal{S}_i|}$ for the FCs of the Fourier-sparse approximation $\tilde{v}_i = F_{\cdot, \mathcal{S}_i}^{-1} w$.

- **WHT:** as already mentioned, for the WHT this is done using the *compressive sensing method* by Stobbe and Krause (2012).
- **FT3 and FT4:** for FT3 and FT4 we cannot use the *compressive sensing method* and instead solve the following least squares problem

$$\min_{w \in \mathbb{R}^{\ell_3}} \sum_{(x, \hat{v}_i(x)) \in R_i} \left(\hat{v}_i(x) - \underbrace{\left(F_{\cdot, \mathcal{S}_i}^{-1} w \right)(x)}_{=\tilde{v}_i(x)} \right)^2.$$

In Figure 3, we present a flow diagram of the different algorithms we use in HYBRID ICA.

D.2 Details of Experiments

In Figures 4–5, we present detailed efficiency results of HYBRID ICA in all three SATS domains, where we used the best found configuration of hyperparameters from Table 4.

In the upper plot we show in each figure the efficiency of the different phases of HYBRID ICA.⁸ In the lower plot, we present a histogram of the final efficiency distribution over 100 (in GSVM and LSVM) and 30 (in MRVM) new CA instances.

	NNs Architecture	FT	ℓ_1	ℓ_2	ℓ_3	ℓ_4
GSVM	R:[32, 32] N:[10, 10]	WHT	30	21	20	29
LSVM	R:[32, 32] N:[10, 10, 10]	WHT	30	30	10	30
MRVM	L,R,N:[16, 16]	FT4	30	220	100	150

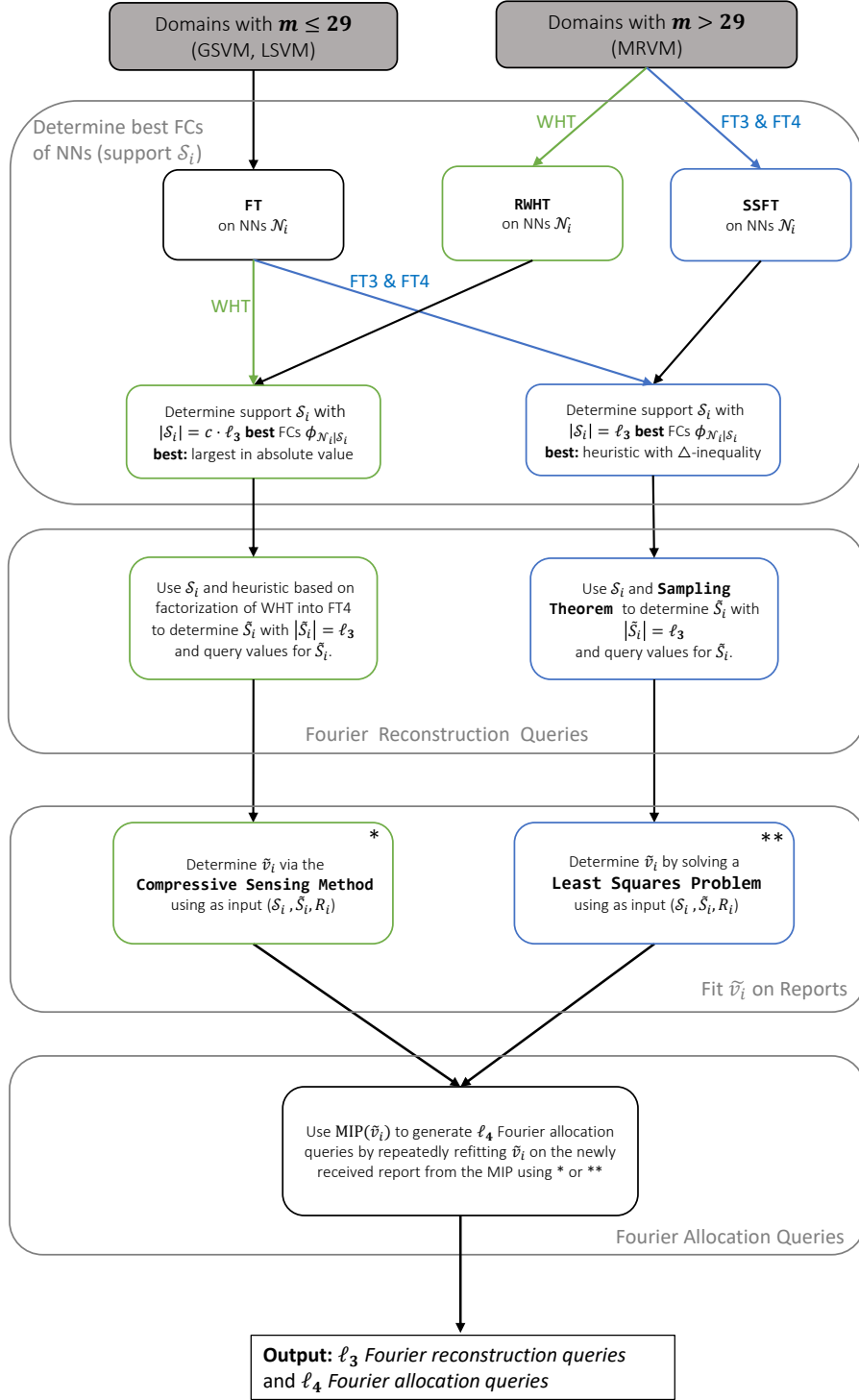
Table 4: Best configuration of HYBRID ICA.

GSVM (Figure 4) We again reprint the efficiency results of the different paths of HYBRID ICA for GSVM, which is discussed in detail in the main paper. Furthermore, we present in the lower plot a histogram of the final efficiency distribution. We see, that for 65 out of 100 instances HYBRID ICA impressively achieves an economic efficiency of 100% using in total only 100 value queries per bidder.

LSVM (Figure 5) Starting with $\ell_1 = 30$ random initial queries, HYBRID ICA achieves an average efficiency of approximately 62%. Next, HYBRID ICA performs 5 MLCA iterations. After these 5 MLCA iterations, HYBRID ICA already found for each of the 100 instances an allocation with an efficiency of at least 80% with an average efficiency of 98%. Here, in the non-sparse LSVM domain, the *Fourier reconstruction and allocation queries* can only slightly increase the efficiency of some outliers arriving at an average efficiency of 98.47%. In the histogram, we see, that for 58 instances, HYBRID ICA was able to achieve full efficiency. Overall, we observe, that in the non-sparse LSVM the Fourier-based approach is not as effective as in the sparse GSVM, but still leads to results, that statistically match the efficiency of MLCA (see Table 3 in the main paper).

MRVM (Figure 6) Starting with $\ell_1 = 30$ random initial queries, HYBRID ICA achieves an average efficiency of approximately 50%. Next, HYBRID ICA performs 55 MLCA iterations and asks in total 220 *MLCA allocation queries*. Here, we observe a steep increase in efficiency at the beginning. In later iterations the increase in efficiency gets smaller resulting in an average efficiency of 94.34%. In MRVM, we do not observe an increase in efficiency using the $\ell_3 = 100$ *Fourier-based reconstruction queries*. However, the $\ell_4 = 150$ *Fourier-based allocation queries* significantly increase the efficiency further by 1.38% resulting in an final average efficiency of 95.72%.

⁸In MRVM we abbreviate the different query types as follows: RI=random initial queries, 1-55=MLCA iterations, FR=Fourier reconstruction queries, FA=Fourier allocation queries.



Algorithms:

FT: (Full) Fourier transform, Püschel and Wendler (2020).

RWHT: Robust sparse WHT algorithm, Amrollahi et al. (2019).

SSFT: Sparse set function Fourier transform, Anonymous (2020)

Sampling Theorem: Püschel and Wendler (2020).

Compressive Sensing Method: Stobbe and Krause (2012).

Figure 3: Overview of Fourier Transform-based Procedures in HYBRID ICA.

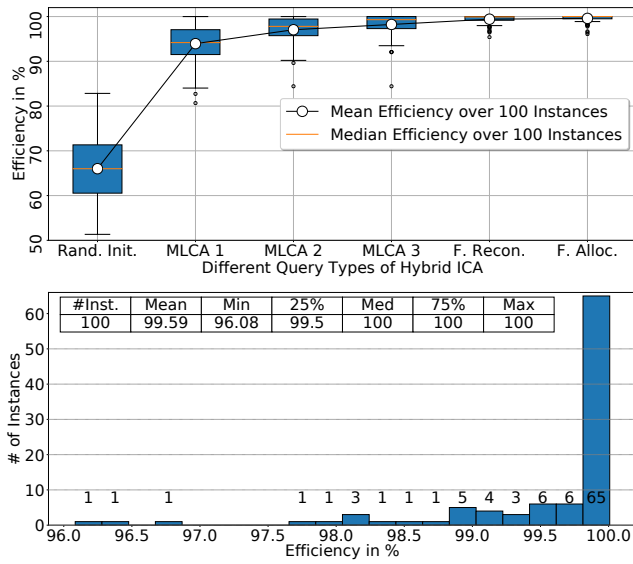


Figure 4: Details of HYBRID ICA in GSVM.

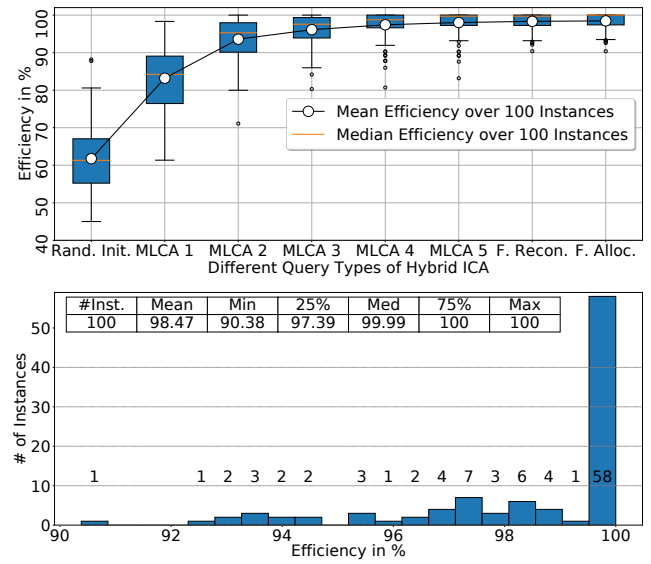


Figure 5: Details of HYBRID ICA in LSVM.

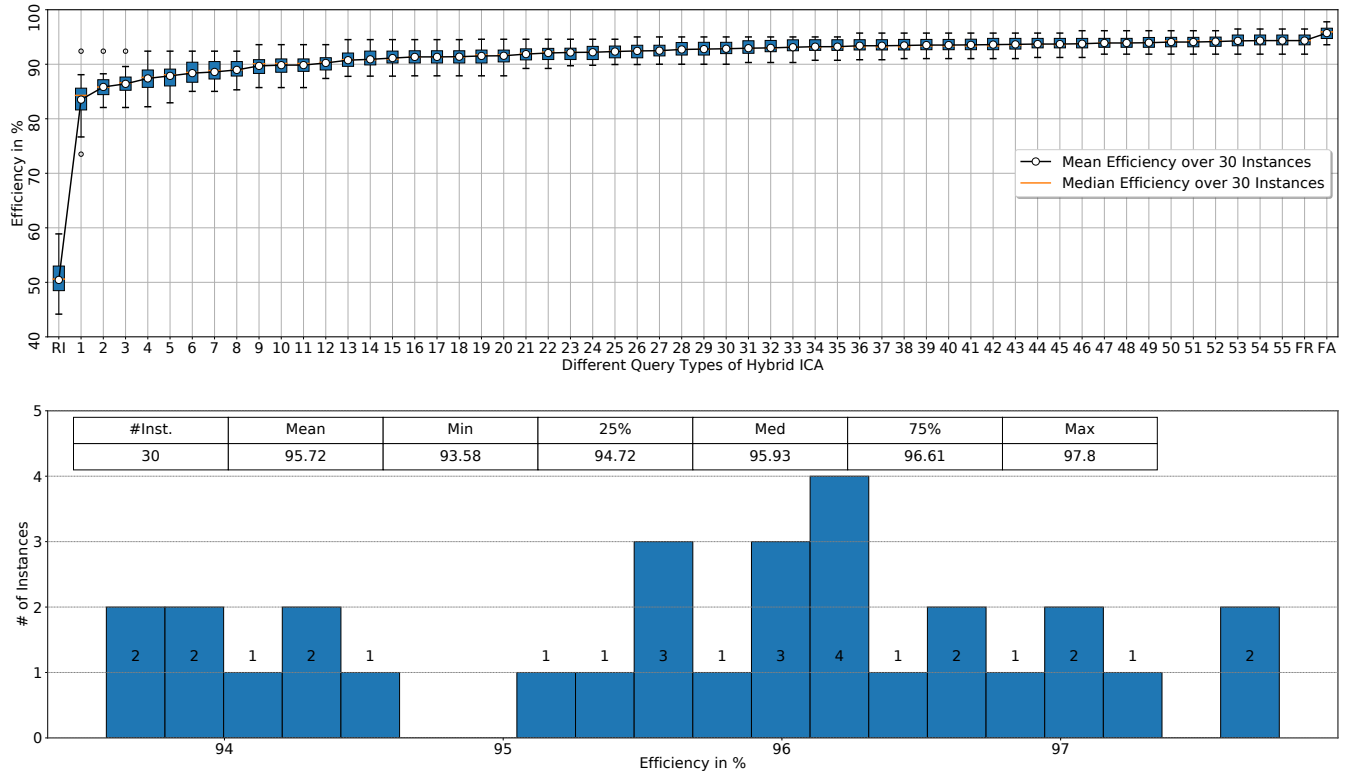


Figure 6: Details of HYBRID ICA in MRVM.